



Markus Lazar

Reduced strain gradient elasticity model with two characteristic lengths: fundamentals and application to straight dislocations

Received: 6 June 2022 / Accepted: 30 June 2022
© The Author(s) 2022

Abstract In this paper, the reduced strain gradient elasticity model with two characteristic lengths is proposed and presented. The reduced strain gradient elasticity model is a particular case of Mindlin's first strain gradient elasticity theory with a reduced number of material parameters and is a generalization of the simplified first strain gradient elasticity model to include two different characteristic length scale parameters. The two characteristic lengths have the physical meaning of longitudinal and transverse length scales. The reduced strain gradient elasticity model is used to study screw and edge dislocations and to derive analytical solutions of the dislocation fields. The displacement, elastic distortion, plastic distortion and Cauchy stress fields of screw and edge dislocations are non-singular, finite and smooth. The dislocation fields of a screw dislocation depend on one characteristic length, whereas the dislocation fields of an edge dislocation depend on up to two characteristic lengths. For the numerical analysis of the dislocation fields, the material parameters including the characteristic lengths have been used, computed from a second nearest neighbor modified embedded-atom method (2NN MEAM) potential for aluminum.

Keywords Gradient elasticity · Dislocations · Plastic distortion · Dislocation density · Regularization

1 Introduction

It is well known that classical elasticity theory is not valid at small scales and leads to unphysical singularities at small scales. For instance, the (classical) stress and elastic strain fields of screw and edge dislocations possess a $1/r$ -singularity (see, e.g., [12,34,39]). On the other hand, generalized continuum theories such as strain gradient elasticity and nonlocal elasticity are continuum theories valid at small scales (see, e.g., [8,29,31]). In particular, Mindlin [36] (see also [37]) developed the theory of first strain gradient elasticity which is a powerful theory. In first strain gradient elasticity, the elastic energy density depends on the gradient of the elastic strain tensor in addition to the elastic strain tensor. Due to the strain gradients, strain gradient elasticity possesses a weak nonlocality important for the mathematical modeling of crystals in the framework of generalized continua. Isotropic first strain gradient elasticity theory contains two Lamé constants and five strain gradient parameters leading to two characteristic lengths.

Toupin and Grazis [47] and Mindlin [38] (see also [13]) showed that first strain gradient elasticity, which is sometimes called gradient elasticity of grade-2, can be considered as the continuum version of a lattice theory with up to second-neighbor interactions (nearest and next-nearest neighbor interactions). Therefore, a second nearest neighbor interatomic potential should be used for the computation of material parameters in first

Communicated by Andreas Öchsner.

M. Lazar (✉)
Institute of Engineering Mechanics, Karlsruhe Institute of Technology (KIT), 76131 Karlsruhe, Germany
E-mail: markus.lazar@kit.edu

strain gradient elasticity. Nowadays, it has been understood that strain gradient elasticity is a straightforward continuum theory for mechanics at small scales. Using ab initio density functional theory (DFT) calculations, Shodja et al. [45] showed that the two characteristic lengths of Mindlin's isotropic strain gradient elasticity theory are in the order of $\sim 10^{-10}$ m (Ångström) for several fcc and bcc materials. The size of the characteristic lengths gives the information where the weak nonlocality of strain gradient elasticity is dominant. Therefore, the weak nonlocality is dominant in strain gradient elasticity at the Ångström-scale. All material parameters of first strain gradient elasticity can be computed using interatomic potentials [1,31,43]. In particular, the atomistic representation of the constitutive tensors in first strain gradient elasticity has been given by Admal et al. [1].

Let us note that in the early days of gradient elasticity, several trials (e.g., [16,44]) to find non-singular fields produced by dislocations were not successful, leading only to additional singularities in the dislocation fields. More than three decades later, Altan and Aifantis [3] have derived a simplified version of Mindlin's first strain gradient elasticity. Using such a simplified first strain gradient elasticity with only one characteristic length scale parameter, Gutkin and Aifantis [9,10] found, for the first time, non-singular elastic strain fields of screw and edge dislocations. Lazar and Maugin [19] (see also [20,27]) have shown how non-singular stress and strain fields of screw and edge dislocations can be computed in simplified first strain gradient elasticity. Such simplified first strain gradient elasticity is a particular version of Mindlin's first strain gradient elasticity where the double stress tensor can be expressed in terms of the gradient of the Cauchy stress tensor (see, e.g., [19,26]). An important mathematical property of strain gradient elasticity is that it provides a mathematical regularization based on partial differential equations (PDEs) of higher order where the characteristic length scale parameter plays the role of the regularization parameter. Using an incompatible version of Mindlin's first strain gradient elasticity, non-singular and smooth displacement fields of screw and edge dislocations have been recently given by Delfani and Tavakol [4] and Delfani et al. [5], respectively. All non-singular dislocation fields including elastic strain, stress, and displacement fields of screw and edge dislocations have been derived by Lazar [30] in the framework of incompatible first strain gradient elasticity of Mindlin type.

The main disadvantage of simplified first strain gradient elasticity is that it possesses only one characteristic length scale in addition to the two Lamé constants in contrast to Mindlin's first strain gradient elasticity which possesses two characteristic length scales for the isotropic case. As a consequence, the elastic shear strain (deviatoric part of the elastic strain tensor) and elastic dilatation (spherical part of the elastic strain tensor) have the same characteristic length scale, which is to some degree unphysical because shear strain and dilatation are the two irreducible pieces of the elastic strain tensor or the two eigen-modes (see [27]). To be more physical, at least every eigen-mode or every Lamé constant should have its own independent characteristic length scale. On the other hand, Mindlin's first strain gradient elasticity with its five gradient-elastic constants is sometimes too complicated and sophisticated for applications. For that reason, we want to derive the reduced strain gradient elasticity model with two characteristic length scale parameters in addition to the two Lamé constants. The reduced strain gradient elasticity model is a robust gradient model similar to the simplified strain gradient model but includes the main properties of Mindlin's strain gradient elasticity like two characteristic length scales. Moreover, the reduced strain gradient elasticity model is the bridge between simplified strain gradient elasticity and Mindlin's first strain gradient elasticity.

The paper is organized as follows. In Sect. 2, we present the reduced strain gradient elasticity model with two characteristic lengths as a particular version of the incompatible strain gradient elasticity of Mindlin type with a reduced number of material parameters. We give the expressions for the three-dimensional and two-dimensional Green tensors together with their decomposition into longitudinal and transverse parts. For aluminum, the material parameters including the characteristic lengths have been computed based on a second nearest neighbor modified embedded-atom method (2NN MEAM) interatomic potential. Exact analytical solutions of screw and edge dislocations are given in Sects. 3.1 and 3.2, respectively. In Sect. 3.3, the limit to simplified strain gradient elasticity is shown and performed. Moreover, the comparison of the dislocation fields in reduced strain gradient elasticity, Mindlin's strain gradient elasticity and simplified strain gradient elasticity is given and similarities and differences are pointed out. Conclusions are given in Sect. 4.

2 Incompatible strain gradient elasticity

In this section, we develop the reduced strain gradient elasticity model in the framework of incompatible strain gradient elasticity of Mindlin type. First, we present the basics of incompatible strain gradient elasticity of Mindlin type. In the second part, the reduced strain gradient elasticity model is derived and presented.

2.1 Mindlin's first strain gradient elasticity

In Mindlin's theory of first strain gradient elasticity [36,37] (see also [28]), the strain energy density for an isotropic materials is given by

$$\mathcal{W}(\mathbf{e}, \nabla \mathbf{e}) = \frac{1}{2} \mathbb{C}_{ijkl} e_{ij} e_{kl} + \frac{1}{2} \mathbb{D}_{ijmkl n} \partial_m e_{ij} \partial_n e_{kl}. \quad (1)$$

The isotropic constitutive tensor of rank four reads as

$$\mathbb{C}_{ijkl} = \lambda \delta_{ij} \delta_{kl} + \mu (\delta_{ik} \delta_{jl} + \delta_{il} \delta_{jk}), \quad (2)$$

where λ and μ are the Lamé moduli (elastic constants) and δ_{ij} is the Kronecker symbol. The isotropic constitutive tensor of rank six reads as

$$\begin{aligned} \mathbb{D}_{ijmkl n} = & \frac{a_1}{2} (\delta_{ij} \delta_{km} \delta_{ln} + \delta_{ij} \delta_{kn} \delta_{lm} + \delta_{kl} \delta_{im} \delta_{jn} + \delta_{kl} \delta_{in} \delta_{jm}) + 2a_2 \delta_{ij} \delta_{kl} \delta_{mn} \\ & + \frac{a_3}{2} (\delta_{jk} \delta_{im} \delta_{ln} + \delta_{ik} \delta_{jm} \delta_{ln} + \delta_{il} \delta_{jm} \delta_{kn} + \delta_{jl} \delta_{im} \delta_{kn}) + a_4 (\delta_{il} \delta_{jk} + \delta_{ik} \delta_{jl}) \delta_{mn} \\ & + \frac{a_5}{2} (\delta_{jk} \delta_{in} \delta_{lm} + \delta_{ik} \delta_{jn} \delta_{lm} + \delta_{jl} \delta_{km} \delta_{in} + \delta_{il} \delta_{km} \delta_{jn}), \end{aligned} \quad (3)$$

where a_1, a_2, a_3, a_4, a_5 are the five strain gradient parameters (gradient-elastic constants) in Mindlin's isotropic first strain gradient elasticity theory [36] (see also [28,31,37]). The incompatible elastic strain tensor e_{ij} reads as

$$e_{ij} = \frac{1}{2} (\beta_{ij} + \beta_{ji}), \quad (4)$$

which is given by the symmetric part of the incompatible elastic distortion tensor

$$\beta_{ij} = \partial_j u_i - \beta_{ij}^P. \quad (5)$$

The incompatible elastic distortion tensor (5) is nothing but the gradient of the displacement vector u_i minus the plastic distortion (or eigendistortion) tensor β_{ij}^P . Note that we use the following abbreviation for the partial derivative: $\partial_j = \partial / \partial x_j$.

In dislocation theory, the dislocation density tensor is defined in terms of the incompatible plastic distortion tensor (see, e.g., [15,25])

$$\alpha_{ij} = -\epsilon_{jkl} \partial_k \beta_{il}^P \quad (6)$$

and may also be expressed in terms of the incompatible elastic distortion tensor

$$\alpha_{ij} = \epsilon_{jkl} \partial_k \beta_{il}, \quad (7)$$

where ϵ_{jkl} indicates the Levi-Civita tensor. Moreover, the dislocation density tensor satisfies the Bianchi identity of dislocations

$$\partial_j \alpha_{ij} = 0, \quad (8)$$

which means that dislocations cannot end inside the body.

The Cauchy stress tensor σ_{ij} and the double stress tensor τ_{ijm} are defined by

$$\sigma_{ij} = \frac{\partial \mathcal{W}}{\partial e_{ij}} = \mathbb{C}_{ijkl} e_{kl}, \quad (9)$$

$$\tau_{ijm} = \frac{\partial \mathcal{W}}{\partial (\partial_m e_{ij})} = \mathbb{D}_{ijmkl n} \partial_n e_{kl}. \quad (10)$$

Using Eqs. (2) and (3), the Cauchy stress tensor reads as

$$\sigma_{ij} = \lambda \delta_{ij} e_{ll} + 2\mu e_{ij} \quad (11)$$

and the double stress tensor reads as

$$\begin{aligned}\tau_{ijm} = & \frac{a_1}{2}(\delta_{im}\partial_j e_{ll} + \delta_{jm}\partial_i e_{ll} + 2\delta_{ij}\partial_l e_{lm}) + 2a_2\delta_{ij}\partial_m e_{ll} \\ & + a_3(\delta_{im}\partial_l e_{jl} + \delta_{jm}\partial_l e_{il}) + 2a_4\partial_m e_{ij} + a_5(\partial_i e_{jm} + \partial_j e_{im}).\end{aligned}\quad (12)$$

In presence of body forces, the (static) Lagrangian density of strain gradient elasticity is given by

$$\mathcal{L} = -\mathcal{W} - \mathcal{V}, \quad (13)$$

where \mathcal{W} is given in Eq. (1) and \mathcal{V} is the potential of body forces given by

$$\mathcal{V} = -u_i f_i. \quad (14)$$

Here f_i denotes the body force density vector. The static (force) equilibrium condition is given by the Euler–Lagrange equation of strain gradient elasticity (see, e.g., [2,35])

$$\frac{\delta \mathcal{L}}{\delta u_i} \equiv \frac{\partial \mathcal{L}}{\partial u_i} - \partial_j \frac{\partial \mathcal{L}}{\partial (\partial_j u_i)} + \partial_m \partial_j \frac{\partial \mathcal{L}}{\partial (\partial_m \partial_j u_i)} = 0. \quad (15)$$

In terms of the Cauchy stress and double stress tensors, the equation of equilibrium (15) takes the following form [36]

$$\partial_j (\sigma_{ij} - \partial_m \tau_{ijm}) = -f_i, \quad (16)$$

which has the physical meaning of the force equilibrium condition. Moreover, the total or effective stress tensor $\widehat{\sigma}_{ij}$ can be defined as a variational derivative

$$\widehat{\sigma}_{ij} := \frac{\delta \mathcal{W}}{\delta e_{ij}} = \frac{\partial \mathcal{W}}{\partial e_{ij}} - \partial_k \frac{\partial \mathcal{W}}{\partial (\partial_k e_{ij})}. \quad (17)$$

Using Eqs. (9) and (10), it reads as (see also [22,28,35,47])

$$\widehat{\sigma}_{ij} = \sigma_{ij} - \partial_m \tau_{ijm} \quad (18)$$

and Eq. (16) reduces to the simple form

$$\partial_j \widehat{\sigma}_{ij} = -f_i. \quad (19)$$

Using Eqs. (11) and (12), the total or effective stress tensor (18) reduces to

$$\begin{aligned}\widehat{\sigma}_{ij} = & 2\mu e_{ij} + \lambda \delta_{ij} e_{ll} - a_1 (\partial_i \partial_j e_{ll} + \partial_k \partial_l \delta_{ij} e_{kl}) - 2a_2 \delta_{ij} \Delta e_{ll} \\ & - (a_3 + a_5) (\partial_i \partial_l e_{jl} + \partial_j \partial_l e_{il}) - 2a_4 \Delta e_{ij},\end{aligned}\quad (20)$$

where Δ denotes the Laplace operator. If we substitute the total stress tensor (20) into Eq. (19), then the displacement equation of equilibrium is given by

$$L_{ik}^M u_k = \mu [1 - \ell_2^2 \Delta] (\partial_l \beta_{il}^P + \partial_l \beta_{li}^P) + [\lambda - (a_1 + 2a_2) \Delta] \partial_i \beta_{ll}^P - (a_1 + a_3 + a_5) \partial_i \partial_k \partial_l \beta_{kl}^P - f_i, \quad (21)$$

where L_{ik}^M denotes the tensorial linear partial differential operator of fourth order, appearing in Mindlin's first strain gradient elasticity, and is called the Mindlin operator. The isotropic Mindlin operator reads as

$$L_{ik}^M = (\lambda + 2\mu) [1 - \ell_1^2 \Delta] \partial_i \partial_k + \mu [1 - \ell_2^2 \Delta] (\delta_{ik} \Delta - \partial_i \partial_k). \quad (22)$$

Note that $L_{ik}^M = L_{ki}^M$. The two characteristic lengths in Mindlin's strain gradient elasticity, defined in terms of the five gradient-elastic constants and the two Lamé constants, are defined by

$$\ell_1^2 = \frac{2(a_1 + a_2 + a_3 + a_4 + a_5)}{\lambda + 2\mu}, \quad (23)$$

$$\ell_2^2 = \frac{a_3 + 2a_4 + a_5}{2\mu}. \quad (24)$$

Using the longitudinal and transverse sound speeds

$$c_L^2 = \frac{\lambda + 2\mu}{\rho}, \quad c_T^2 = \frac{\mu}{\rho}, \quad (25)$$

where ρ denotes the mass density, the Mindlin operator (22) can be decomposed into a longitudinal part and a transverse part and can be rewritten as

$$L_{ik}^M = \rho c_L^2 [1 - \ell_L^2 \Delta] \partial_i \partial_k + \rho c_T^2 [1 - \ell_T^2 \Delta] (\delta_{ik} \Delta - \partial_i \partial_k), \quad (26)$$

namely

$$L_{ik}^M = L_{ik}^{M,L} + L_{ik}^{M,T} \quad (27)$$

with

$$L_{ik}^{M,L} = \rho c_L^2 [1 - \ell_L^2 \Delta] \partial_i \partial_k \quad (28)$$

$$L_{ik}^{M,T} = \rho c_T^2 [1 - \ell_T^2 \Delta] (\delta_{ik} \Delta - \partial_i \partial_k) \quad (29)$$

and the conditions for the longitudinal and transverse parts

$$\epsilon_{lji} \partial_j L_{ik}^{M,L} = 0 \quad (30)$$

$$\partial_i L_{ik}^{M,T} = 0. \quad (31)$$

It can be seen in Eq. (26) that every sound velocity has its own characteristic length. Therefore, the characteristic length ℓ_1 has the physical meaning of characteristic longitudinal length ℓ_L and the characteristic length ℓ_2 has the physical meaning of characteristic transverse length ℓ_T :

$$\ell_1 = \ell_L, \quad \ell_2 = \ell_T. \quad (32)$$

2.2 Reduced strain gradient elasticity model with two characteristic lengths

The reduced strain gradient elasticity model with two characteristic lengths is obtained from Mindlin's isotropic first strain gradient elasticity if we assume to every Lamé constant λ and μ an independent length ℓ_λ and ℓ_μ , which we may call the characteristic lengths of the Lamé constants, via

$$a_1 = 0, \quad a_2 = \frac{\lambda \ell_\lambda^2}{2}, \quad a_3 = 0, \quad a_4 = \mu \ell_\mu^2, \quad a_5 = 0. \quad (33)$$

On the one hand, the reduced strain gradient elasticity model is a particular case of Mindlin's first strain gradient elasticity theory. On the other hand, it is a generalization of the simplified first strain gradient elasticity model to include two different characteristic length scale parameters.

Using the relations in(33), the constitutive tensor of rank six, Eq. (3), reduces to

$$\mathbb{D}_{ijmkl n} = \lambda \ell_\lambda^2 \delta_{ij} \delta_{kl} \delta_{mn} + \mu \ell_\mu^2 (\delta_{il} \delta_{jk} + \delta_{ik} \delta_{jl}) \delta_{mn} \quad (34)$$

and the double stress tensor (12) becomes

$$\tau_{ijm} = \lambda \ell_\lambda^2 \delta_{ij} \partial_m e_{ll} + 2\mu \ell_\mu^2 \partial_m e_{ij}. \quad (35)$$

It is worth noting that the double stress tensor (35) is nothing but the gradient of the Cauchy stress tensor (11) with an independent length scale for every Lamé constant. The double stress tensor (35) is much simpler than the expression of the double stress tensor (12) in Mindlin's strain gradient elasticity. Substituting the constitutive tensors (2) and (34) into Eq. (1), the elastic strain energy density reduces to

$$\mathcal{W}(\mathbf{e}, \nabla \mathbf{e}) = \frac{1}{2} \lambda e_{ii} e_{jj} + \mu e_{ij} e_{ij} + \frac{1}{2} \lambda \ell_\lambda^2 \partial_k e_{ii} \partial_k e_{jj} + \mu \ell_\mu^2 \partial_k e_{ij} \partial_k e_{ij}. \quad (36)$$

By means of Eqs. (11) and (35), the total or effective stress tensor (20) simplifies to

$$\widehat{\sigma}_{ij} = 2\mu[1 - \ell_\mu^2 \Delta]e_{ij} + \lambda[1 - \ell_\lambda^2 \Delta]\delta_{ij}e_{ll}, \quad (37)$$

where it can be seen that every elastic constant possesses its own Helmholtz operator. For the total stress tensor (37) with two independent characteristic length scales, the equation of equilibrium (19) gives in the framework reduced strain gradient elasticity the corresponding displacement equation of equilibrium

$$\begin{aligned} \mu[1 - \ell_\mu^2 \Delta](\Delta u_i + \partial_i \partial_k u_k) + \lambda[1 - \ell_\lambda^2 \Delta]\partial_i \partial_k u_k = & \mu[1 - \ell_\mu^2 \Delta]\partial_l (\beta_{il}^P + \beta_{ii}^P) \\ & + \lambda[1 - \ell_\lambda^2 \Delta]\partial_i \beta_{ll}^P - f_i. \end{aligned} \quad (38)$$

However, sometimes this representation in terms of length scales of the Lamé constants ℓ_λ and ℓ_μ is not very suitable for the investigation of specific gradient phenomena. Consequently, we use a more suitable representation in terms of longitudinal and transverse length scales ℓ_1 and ℓ_2 . Therefore, the following representation is used

$$a_1 = 0, \quad a_2 = \frac{(\lambda + 2\mu)\ell_1^2}{2} - \mu\ell_2^2, \quad a_3 = 0, \quad a_4 = \mu\ell_2^2, \quad a_5 = 0 \quad (39)$$

and the relations between the length scales (ℓ_λ, ℓ_μ) and the longitudinal and transverse length scales (ℓ_1, ℓ_2) read

$$\ell_\mu^2 = \ell_2^2, \quad \ell_\lambda^2 = \frac{\lambda + 2\mu}{\lambda} \ell_1^2 - \frac{2\mu}{\lambda} \ell_2^2 \quad (40)$$

and

$$\ell_1^2 = \frac{\lambda \ell_\lambda^2 + 2\mu \ell_\mu^2}{\lambda + 2\mu}. \quad (41)$$

Substituting Eq. (40) into Eq. (36), the elastic strain energy density can be written as

$$\begin{aligned} \mathcal{W}(\mathbf{e}, \nabla \mathbf{e}) = & \frac{1}{2}(\lambda + 2\mu)e_{ii}e_{jj} + \mu(e_{ij}e_{ij} - e_{ii}e_{jj}) \\ & + \frac{1}{2}(\lambda + 2\mu)\ell_1^2 \partial_k e_{ii} \partial_k e_{jj} + \mu\ell_2^2 (\partial_k e_{ij} \partial_k e_{ij} - \partial_k e_{ii} \partial_k e_{jj}). \end{aligned} \quad (42)$$

Then the constitutive tensor of rank six, Eq. (34), reduces to

$$\mathbb{D}_{ijmkl n} = (\lambda + 2\mu)\ell_1^2 \delta_{ij} \delta_{kl} \delta_{mn} + \mu\ell_2^2 (\delta_{il} \delta_{jk} + \delta_{ik} \delta_{jl} - 2\delta_{ij} \delta_{kl}) \delta_{mn} \quad (43)$$

and the double stress tensor (34) becomes

$$\tau_{ijm} = (\lambda + 2\mu)\ell_1^2 \delta_{ij} \partial_m e_{ll} + 2\mu\ell_2^2 \partial_m (e_{ij} - \delta_{ij} e_{ll}). \quad (44)$$

Moreover, the Cauchy stress tensor (11) can be written in the form

$$\sigma_{ij} = (\lambda + 2\mu)\delta_{ij} e_{ll} + 2\mu(e_{ij} - \delta_{ij} e_{ll}) \quad (45)$$

and the total or effective stress tensor (37) reduces to

$$\widehat{\sigma}_{ij} = (\lambda + 2\mu)[1 - \ell_1^2 \Delta]\delta_{ij} e_{ll} + 2\mu[1 - \ell_2^2 \Delta](e_{ij} - \delta_{ij} e_{ll}). \quad (46)$$

Substituting the total stress tensor (46) into the equation of equilibrium (19), the displacement equation of equilibrium is obtained as

$$\begin{aligned} (\lambda + 2\mu)[1 - \ell_1^2 \Delta]\partial_i \partial_k u_k + \mu[1 - \ell_2^2 \Delta](\Delta u_i - \partial_i \partial_k u_k) = & (\lambda + 2\mu)[1 - \ell_1^2 \Delta]\partial_i \beta_{ll}^P \\ & + \mu[1 - \ell_2^2 \Delta](\partial_l \beta_{il}^P + \partial_l \beta_{ii}^P - 2\partial_i \beta_{ll}^P) - f_i, \end{aligned} \quad (47)$$

which can be written in terms of the Mindlin operator (22)

$$L_{ik}^M u_k = (\lambda + 2\mu)[1 - \ell_1^2 \Delta] \partial_i \beta_{ll}^P + \mu[1 - \ell_2^2 \Delta](\partial_l \beta_{il}^P + \partial_l \beta_{li}^P - 2\partial_i \beta_{ll}^P) - f_i \quad (48)$$

or in terms of longitudinal and transverse length scales and longitudinal and transverse speeds of sound

$$c_L^2[1 - \ell_L^2 \Delta] \partial_i \partial_k u_k + c_T^2[1 - \ell_T^2 \Delta](\Delta u_i - \partial_i \partial_k u_k) = c_L^2[1 - \ell_L^2 \Delta] \partial_i \beta_{ll}^P + c_T^2[1 - \ell_T^2 \Delta](\partial_l \beta_{il}^P + \partial_l \beta_{li}^P - 2\partial_i \beta_{ll}^P) - f_i / \rho. \quad (49)$$

It is important to note that the left-hand side of the displacement equation of equilibrium in Mindlin's strain gradient elasticity (21) and in reduced strain gradient elasticity (48) is formally given by the same type of differential operator, namely the Mindlin operator L_{ik}^M , whereas the right-hand side of the displacement equation of equilibrium is much simpler in reduced strain gradient elasticity than in Mindlin's strain gradient elasticity. In contrast to the right hand side of Eq. (21), the right hand side of Eq. (48) is given in terms of longitudinal and transverse Helmholtz operators. For the compatible case, where the plastic distortion is zero, both equations (21) and (48) reduce to the same partial differential equation, namely

$$L_{ik}^M u_k = -f_i. \quad (50)$$

Moreover, for both Eqs. (21) and (48), the particular solutions can be given by the convolution of the inhomogeneous parts and the Green tensor of the Mindlin operator, which is given in the next section.

2.3 Green tensor of the Mindlin operator

The Green tensor of the isotropic Mindlin operator (22), being the fundamental solution, is defined by (see, e.g., [28])

$$L_{ik}^M G_{kj}^M(\mathbf{R}) = -\delta_{ij} \delta(\mathbf{R}), \quad (51)$$

where $\delta(\cdot)$ denotes the Dirac delta function. Note that the Green tensor is a symmetric tensor: $G_{kj}^M = G_{jk}^M$.

The three-dimensional Green tensor of the Mindlin operator (22) reads as (see [14,28,44])

$$G_{ij}^M(\mathbf{R}) = \frac{1}{8\pi} \left[\frac{1}{\lambda + 2\mu} \partial_i \partial_j A(R, \ell_1) + \frac{1}{\mu} (\delta_{ij} \Delta - \partial_i \partial_j) A(R, \ell_2) \right] \quad (52)$$

with the two scalar auxiliary functions

$$A(R, \ell_1) = R + \frac{2\ell_1^2}{R} (1 - e^{-R/\ell_1}), \quad (53)$$

$$A(R, \ell_2) = R + \frac{2\ell_2^2}{R} (1 - e^{-R/\ell_2}), \quad (54)$$

where $i, j = x, y, z$ and $\mathbf{R} \in \mathbb{R}^3$.

The two-dimensional Green tensor of the plane strain problem in Mindlin's strain gradient elasticity reads as (see [14,28,44])

$$G_{ij}^M(\mathbf{R}) = \frac{1}{8\pi} \left[\frac{1}{\lambda + 2\mu} \partial_i \partial_j A(R, \ell_1) + \frac{1}{\mu} (\delta_{ij} \Delta - \partial_i \partial_j) A(R, \ell_2) \right] \quad (55)$$

with the two scalar auxiliary functions

$$A(R, \ell_1) = -\left(R^2 \ln R - R^2 + 4\ell_1^2 [\ln R + K_0(R/\ell_1)] \right), \quad (56)$$

$$A(R, \ell_2) = -\left(R^2 \ln R - R^2 + 4\ell_2^2 [\ln R + K_0(R/\ell_2)] \right), \quad (57)$$

where $i, j = x, y$ and $\mathbf{R} \in \mathbb{R}^2$. Here K_n is the modified Bessel function of the second kind of order n .

In general, the Green tensor of the Mindlin operator can be decomposed into longitudinal and transverse pieces according to

$$G_{ij}^{\mathbf{M}}(\mathbf{R}) = G_{ij}^{\mathbf{M,L}}(\mathbf{R}) + G_{ij}^{\mathbf{M,T}}(\mathbf{R}), \quad (58)$$

where the longitudinal and transverse Green tensors are given by

$$G_{ij}^{\mathbf{M,L}}(\mathbf{R}) = \frac{1}{8\pi\rho c_L^2} \partial_i \partial_j A(R, \ell_L), \quad (59)$$

$$G_{ij}^{\mathbf{M,T}}(\mathbf{R}) = \frac{1}{8\pi\rho c_T^2} (\delta_{ij} \Delta - \partial_i \partial_j) A(R, \ell_T) \quad (60)$$

with the conditions to be longitudinal and transverse

$$\epsilon_{lkj} \partial_k G_{ij}^{\mathbf{M,L}}(\mathbf{R}) = 0 \quad (61)$$

$$\partial_j G_{ij}^{\mathbf{M,T}}(\mathbf{R}) = 0. \quad (62)$$

For the anti-plane strain problem, the Mindlin operator (22) reduces to the two-dimensional Laplace–Helmholtz operator depending only on the length ℓ_2

$$L_{zz}^{\mathbf{M}} = \mu[1 - \ell_2^2 \Delta] \Delta. \quad (63)$$

The corresponding Green function of anti-plane strain is defined by (see, e.g., [28])

$$L_{zz}^{\mathbf{M}} G_{zz}^{\mathbf{M}}(\mathbf{R}) = -\delta(\mathbf{R}) \quad (64)$$

and reads as (see [28])

$$G_{zz}^{\mathbf{M}}(\mathbf{R}) = -\frac{1}{2\pi\mu} [\ln R + K_0(R/\ell_2)]. \quad (65)$$

Moreover, the two-dimensional Green function of the Helmholtz operator is needed in problems of straight dislocations and is defined by

$$L_I G^{L_I} = \delta(\mathbf{R}), \quad I = 1, 2 \quad (66)$$

and reads as

$$G^{L_I} = \frac{1}{2\pi\ell_I^2} K_0(R/\ell_I), \quad (67)$$

where the isotropic scalar Helmholtz operator (differential operator of second order) reads

$$L_I = 1 - \ell_I^2 \Delta, \quad \ell_I > 0. \quad (68)$$

Sometimes in the mathematical literature, the differential operator (68) is called modified Helmholtz operator [48] or metaharmonic operator [40].

Table 1 Lamé moduli, gradient-elastic constants, characteristic lengths, equilibrium lattice parameter, and Poisson ratio for aluminum (Al) computed from 2NN MEAM interatomic potential [31]

λ (eV/Å ³)	μ (eV/Å ³)	a_1 (eV/Å)	a_2 (eV/Å)	a_3 (eV/Å)	a_4 (eV/Å)	a_5 (eV/Å)
0.38649	0.19704	-0.13862	0.22500	0.10877	0.15309	0.21632
ℓ_1 (Å)	ℓ_2 (Å)	ℓ (Å)	a (Å)	ν		
1.2027	1.2657	1.1300	4.05	0.3312		

2.4 Material parameters

In Mindlin's first strain gradient elasticity theory, the elastic constants and the gradient-elastic constants are characteristic material parameters which can be computed from interatomic potentials (see, e.g., [1, 43]) or via ab DFT calculations (see, e.g., [46]). For some important cubic materials such as Al, Cu, Fe and W, the 3 elastic constants and 11 gradient-elastic constants have been computed using the second nearest neighbor modified embedded-atom-method (2NN MEAM) interatomic potential given by Lee et al.[32] (see [1, 31, 33, 43]). Although W and Al are nearly isotropic concerning the elastic constants because they satisfy the isotropy condition for the constitutive tensor of rank 4, \mathbb{C}_{ijkl} , the 11 gradient-elastic constants of W and Al do not satisfy any of the 6 isotropy conditions for the constitutive tensor of rank 6, \mathbb{D}_{ijmklm} , as shown in [31]. Based on the Hermann theorem, the rank 6 of the constitutive tensor \mathbb{D}_{ijmklm} is too high for a crystal possessing a cubic symmetry to be isotropic [31]. Therefore, an average of the gradient-elastic constants of cubic materials is necessary to get isotropic gradient-elastic constants. Lazar et al.[31] proposed and used a Voigt-type average of the sixth-rank constitutive tensor \mathbb{D}_{ijmklm} for the computation of the 5 isotropic gradient-elastic constants (a_1, a_2, a_3, a_4, a_5) of Al and W.

For the numerical analysis of the dislocation fields produced by screw and edge dislocations we choose aluminum (Al) and we use the corresponding Lamé moduli (μ, λ) and the 5 gradient-elastic constants (a_1, a_2, a_3, a_4, a_5) given in [31]. The Lamé constants, gradient-elastic constants, characteristic lengths, and the Poisson ratio of aluminum, which have been computed from the 2NN MEAM interatomic potential [31], are given in Table 1. The 2 characteristic lengths are given in terms the 2 Lamé moduli (μ, λ) and the 5 gradient-elastic constants (a_1, a_2, a_3, a_4, a_5) by Eqs. (23) and (24).

Even for the so-called simplified first strain gradient elasticity theory possessing only 1 characteristic length for isotropic and cubic materials, the characteristic length can be computed directly from the fourth-rank constitutive tensor \mathbb{C}_{ijkl} and the sixth-rank constitutive tensor \mathbb{D}_{ijmklm} by means of a projection method [42] leading to the formula for the characteristic length:

$$\ell^2 = \frac{1}{18} \mathbb{C}_{ijkl}^{-1} \mathbb{D}_{ijmklm} \quad (69)$$

with the inverse tensor of elastic constants for an isotropic material

$$\mathbb{C}_{ijkl}^{-1} = \frac{1}{4\mu} \left(\delta_{ik} \delta_{jl} + \delta_{il} \delta_{jk} - \frac{2\lambda}{3\lambda + 2\mu} \delta_{ij} \delta_{kl} \right). \quad (70)$$

If we substitute Eqs. (3) and (70) into Eq. (69), then we obtain the following formula for the characteristic length in terms of the 2 Lamé moduli (μ, λ) and the 5 gradient-elastic constants (a_1, a_2, a_3, a_4, a_5)

$$\ell^2 = \frac{2\mu(a_1 + 3a_2) + (5\lambda + 4\mu)(a_3 + 3a_4 + a_5)}{6\mu(3\lambda + 2\mu)}. \quad (71)$$

Eq. (71) gives an atomistic determination of the characteristic length ℓ of simplified first strain gradient elasticity from the numerical values of the elastic and gradient elastic constants computed from interatomic potentials or via ab initio DFT. Using the elastic and gradient-elastic constants of Al given in Table 1, the characteristic length ℓ is computed using Eq. (71) and reported in Table 1. It can be seen that for aluminum the length ℓ of simplified strain gradient elasticity is a slightly smaller than the 2 characteristic lengths of Mindlin's strain gradient elasticity theory but in the same size-range.

The size of the characteristic lengths tells us where (weak) nonlocality in gradient theories is dominant. As it can be seen in Table 1, nonlocality is dominant in strain gradient elasticity theory at the Ångström-scale, where classical elasticity theory breaks down and leads to unphysical singularities. In other words,

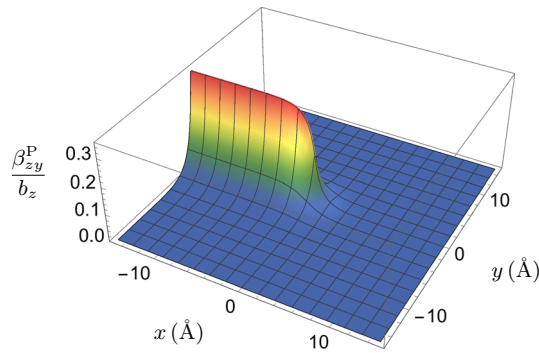


Fig. 1 Plastic distortion β_{zy}^P of a screw dislocation near the dislocation line

the Ångström-scale is the scale of nonlocality in strain gradient elasticity. Strain gradient elasticity becomes relevant at small distances in materials such as crystals. It seems that nonlocality is a fundamental property of nature at small scales. Therefore, strain gradient elasticity is a straightforward continuum theory valid at small scales like the Ångström-scale leading to a straightforward non-singular dislocation theory with non-singular dislocation fields in the dislocation core region as it will be shown in the next section.

3 Application of reduced strain gradient elasticity to straight dislocations

In this section, we investigate the anti-plane strain and plane strain problems of screw and edge dislocations, respectively, in the framework of incompatible reduced strain gradient elasticity for vanishing body force density $f_i = 0$. For the numerical study of the dislocation fields, the elastic constants and the characteristic length scales of aluminum given in Table 1 are used.

3.1 Screw dislocation

The screw dislocation is located at the position $(x, y) = (0, 0)$ with Burgers vector b_z and the dislocation line in the z -direction of a Cartesian coordinate system. For a screw dislocation, Eq. (48) simplifies to

$$L_{zz}^M u_z = \mu L_2 \partial_y \beta_{zy}^P \quad (72)$$

with

$$L_2 \beta_{zy}^P = \beta_{zy}^{P,0} \quad (73)$$

and

$$L_{zz}^M u_z = \mu \partial_y \beta_{zy}^{P,0}. \quad (74)$$

The classical plastic distortion of a screw dislocation given by deWit [6] (see also [39]) reads

$$\beta_{zy}^{P,0} = b_z \delta(y) H(-x) = b_z \delta(y) \int_x^\infty \delta(X) dX, \quad (75)$$

which possesses a discontinuity at $y = 0$ for $x < 0$. Here $H(\cdot)$ denotes the Heaviside step function.

By substituting Eq. (75) into Eq. (73) and using the Green function (67), the plastic distortion is calculated as

$$\beta_{zy}^P = G^{L_2} * \beta_{zy}^{P,0} = \frac{b_z}{2\pi \ell_2^2} \int_x^\infty K_0(\sqrt{X^2 + y^2}/\ell_2) dX, \quad (76)$$

which is non-singular, smooth and finite as it can be seen in Fig. 1. The symbol $*$ denotes spatial convolution.

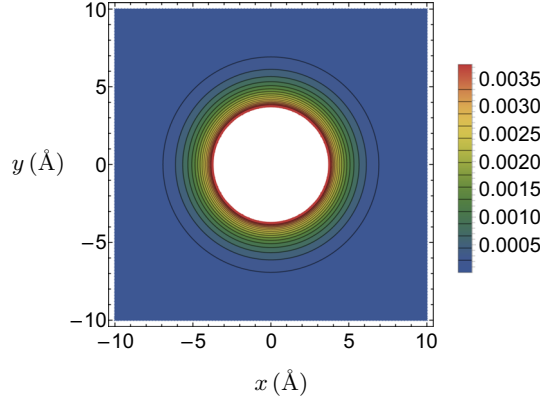


Fig. 2 Contour plot of the dislocation density of a screw dislocation α_{zz} (normalized by the Burgers vector b_z)

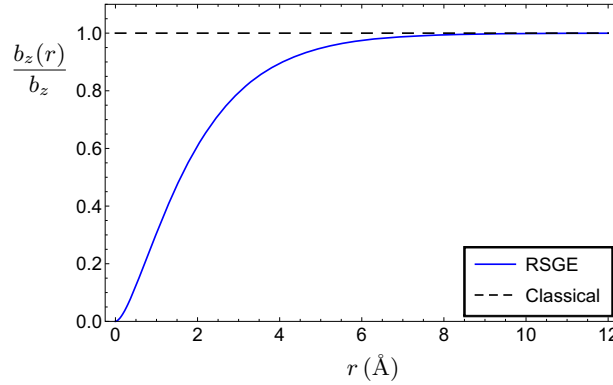


Fig. 3 Effective Burgers vector $b_z(r)$ of a screw dislocation (normalized by the Burgers vector b_z)

The dislocation density of a screw dislocation is obtained as

$$\alpha_{zz} = -\partial_x \beta_{zy}^P = \frac{b_z}{2\pi\ell_2^2} K_0(r/\ell_2), \quad (77)$$

where $r = \sqrt{x^2 + y^2}$. The dislocation density (77) is plotted in Fig. 2 and gives the shape and size of the dislocation core of a screw dislocation.

Using the dislocation density (77), the effective Burgers vector $b_z(r)$ of a screw dislocation is defined by (see, e.g., [7, 17, 18, 23])

$$b_z(r) = \int_0^{2\pi} \int_0^r \alpha_{zz}(r') r' dr' d\phi = b_z \left[1 - \frac{r}{\ell_2} K_1(r/\ell_2) \right]. \quad (78)$$

The effective Burgers vector differs appreciably from the classical Burgers vector b_z , which is constant, in the region from $r = 0$ up to $r \simeq 6\ell_2$. Thus, it is suggestive to take $r_c \simeq 6\ell_2$ as the dislocation core radius. Outside this dislocation core region, the effective Burgers vector reaches its constant value b_z . Accordingly, the gradient solution approaches the classical one outside the dislocation core region. Using the values given in Table 1, the dislocation core radius reads for aluminum: $r_c \simeq 1.875 a = 7.594 \text{ \AA}$. The effective Burgers vector (78) is plotted in Fig. 3.

If we substitute Eq. (75) into Eq. (74) and use the Green function (65), the displacement field u_z is calculated as

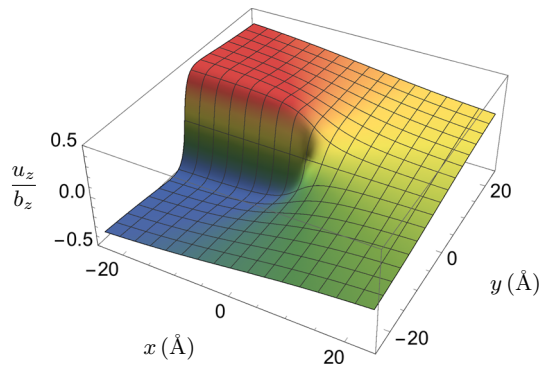


Fig. 4 Displacement field u_z of a screw dislocation near the dislocation line

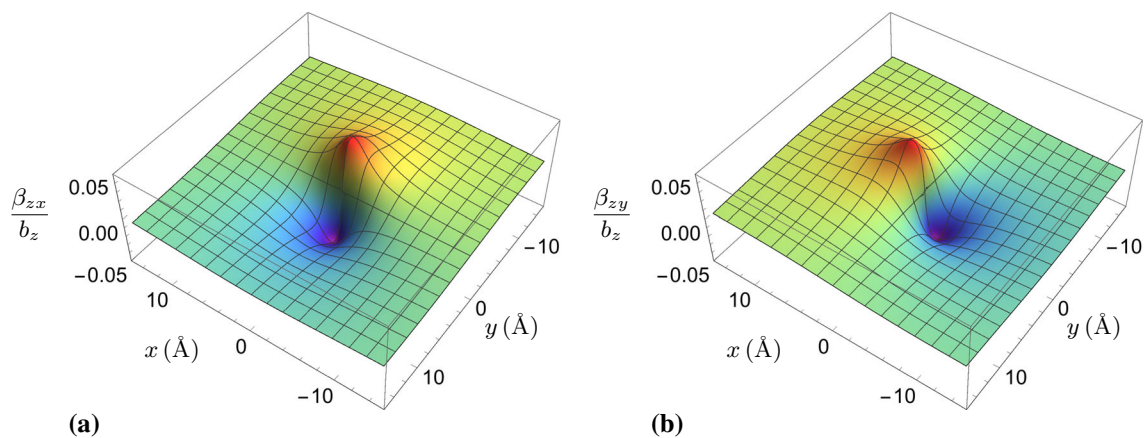


Fig. 5 Elastic distortion components of a screw dislocation near the dislocation line: **a** β_{zx} and **b** β_{zy}

$$\begin{aligned}
 u_z &= -\mu \partial_y G_{zz}^M * \beta_{zy}^{P,0} \\
 &= -\frac{b_z}{2\pi} \partial_y \int_x^\infty \left[\ln \sqrt{X^2 + y^2} + K_0(\sqrt{X^2 + y^2}/\ell_2) \right] dX \\
 &= \frac{b_z}{2\pi} \left(\arctan \frac{y}{x} + \pi H(-x) \operatorname{sgn}(y) + \partial_y \int_x^\infty K_0(\sqrt{X^2 + y^2}/\ell_2) dX \right), \quad (79)
 \end{aligned}$$

where the first part in Eq. (79) is the angle φ with range $(-\pi, \pi]$ and discontinuity of 2π across the negative x -axis (see also [6,41])

$$\varphi = \arctan \frac{y}{x} + \pi H(-x) \operatorname{sgn}(y). \quad (80)$$

The displacement field (79) is plotted in Fig. 4. The displacement field (79) is non-singular and has a smooth form due to the superposition of the classical jump discontinuity (first term) and the gradient term (second term).

The two non-vanishing components of the elastic distortion are calculated as

$$\beta_{zx} = \mu b_z \partial_y G_{zz}^M = -\frac{b_z}{2\pi} \frac{y}{r^2} \left[1 - \frac{r}{\ell_2} K_1(r/\ell_2) \right], \quad (81)$$

$$\beta_{zy} = -\mu b_z \partial_x G_{zz}^M = \frac{b_z}{2\pi} \frac{x}{r^2} \left[1 - \frac{r}{\ell_2} K_1(r/\ell_2) \right]. \quad (82)$$

The two components of the elastic distortion tensor, Eqs. (81) and (82), are plotted in Fig. 5a, b. It can be seen that they are non-singular. The corresponding two non-vanishing components of the non-singular stress tensor simply read

$$\sigma_{zx} = -\frac{\mu b_z}{2\pi} \frac{y}{r^2} \left[1 - \frac{r}{\ell_2} K_1(r/\ell_2) \right], \quad (83)$$

$$\sigma_{zy} = \frac{\mu b_z}{2\pi} \frac{x}{r^2} \left[1 - \frac{r}{\ell_2} K_1(r/\ell_2) \right]. \quad (84)$$

All the dislocation fields obtained in reduced strain gradient elasticity are in agreement with the dislocation fields obtained in Mindlin's strain gradient elasticity (see [4,30]).

3.2 Edge dislocation

The edge dislocation of glide-mode is located at the position $(x, y) = (0, 0)$ with Burgers vector b_x . The dislocation line coincides with the z -axis of a Cartesian coordinate system. For an edge dislocation of glide-mode with Burgers vector b_x , Eq. (48) reduces to

$$L_{ik}^M u_k = \mu L_2 \partial_l (\beta_{il}^P + \beta_{li}^P) \quad (85)$$

with

$$L_2 \beta_{ij}^P = \beta_{ij}^{P,0}, \quad i \neq j \quad (86)$$

and

$$L_{ik}^M u_k = \mu \partial_l (\beta_{il}^{P,0} + \beta_{li}^{P,0}). \quad (87)$$

The classical plastic distortion of an edge dislocation of glide-mode given by deWit [6] (see also [39]) reads

$$\beta_{xy}^{P,0} = b_x \delta(y) H(-x) = b_x \delta(y) \int_x^\infty \delta(X) dX. \quad (88)$$

Substituting Eq. (88) into Eq. (86), the plastic distortion of an edge dislocation is calculated as

$$\beta_{xy}^P = G^{L_2} * \beta_{xy}^{P,0} = \frac{b_x}{2\pi \ell_2^2} \int_x^\infty K_0(\sqrt{X^2 + y^2/\ell_2}) dX \quad (89)$$

and the corresponding dislocation density is obtained as

$$\alpha_{xz} = -\partial_x \beta_{xy}^P = \frac{b_x}{2\pi \ell_2^2} K_0(r/\ell_2). \quad (90)$$

The plastic distortion (89) is non-singular and finite as it can be seen in Fig. 6. The dislocation density (90) is plotted in Fig. 7 and gives the shape and size of the dislocation core of the edge dislocation. Note that in reduced strain gradient elasticity, the plastic distortion (89) and dislocation density (90) of an edge dislocation have the same form as the corresponding fields (76) and (77) of a screw dislocation. The dislocation cores of screw and edge dislocations possess a cylindrical symmetry (see Figs. (2) and (7)) and have the same shape and size in the reduced strain gradient elasticity model.

Using the dislocation density (90), the effective Burgers vector $b_x(r)$ of an edge dislocation is given by

$$b_x(r) = \int_0^{2\pi} \int_0^r \alpha_{xz}(r') r' dr' d\phi = b_x \left[1 - \frac{r}{\ell_2} K_1(r/\ell_2) \right]. \quad (91)$$

This effective Burgers vector differs appreciably from the classical Burgers vector b_x , which is constant, in the region from $r = 0$ up to $r \simeq 6\ell_2$. Note that the effective Burgers vector (91) of an edge dislocation has the same form as the effective Burgers vector (78) of a screw dislocation. The effective Burgers vector (91) is plotted in Fig. 8.

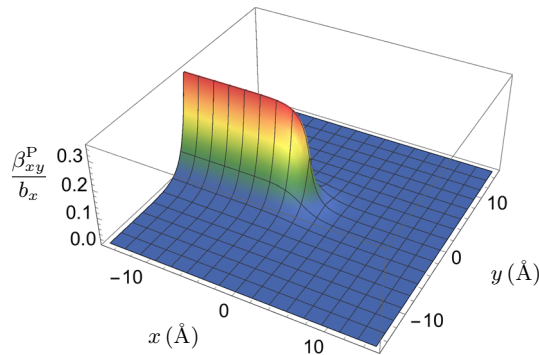


Fig. 6 Plastic distortion β_{xy}^P of an edge dislocation near the dislocation line

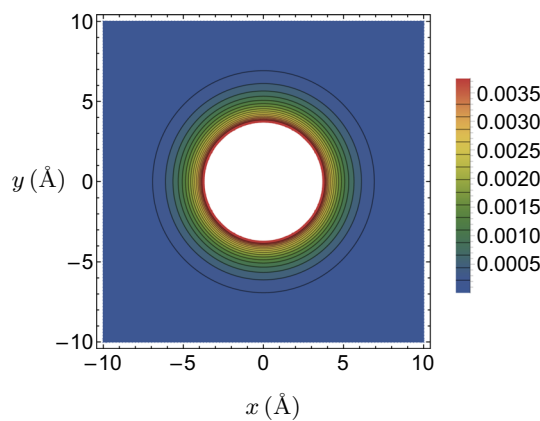


Fig. 7 Contour plot of the dislocation density of an edge dislocation α_{xz} (normalized by the Burgers vector b_x)

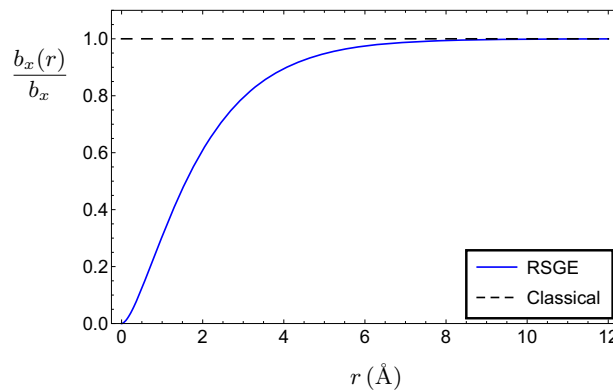


Fig. 8 Effective Burgers vector $b_x(r)$ of an edge dislocation (normalized by the Burgers vector b_x)

The solution of Eq. (87) provides the displacement field of the edge dislocation in the following form

$$u_x = \mu \left(G_{xy}^M * \alpha_{xz}^0 - \partial_y G_{xx}^M * \beta_{xy}^{P,0} \right), \quad (92)$$

$$u_y = \mu \left(G_{yy}^M * \alpha_{xz}^0 - \partial_y G_{yx}^M * \beta_{xy}^{P,0} \right), \quad (93)$$

where $\alpha_{xz}^0 = -\partial_x \beta_{xy}^{P,0} = b_x \delta(x) \delta(y)$ is the classical dislocation density of an edge dislocation. Substituting the classical plastic distortion and the Green tensor (55) into Eqs. (92) and (93), a straightforward calculation

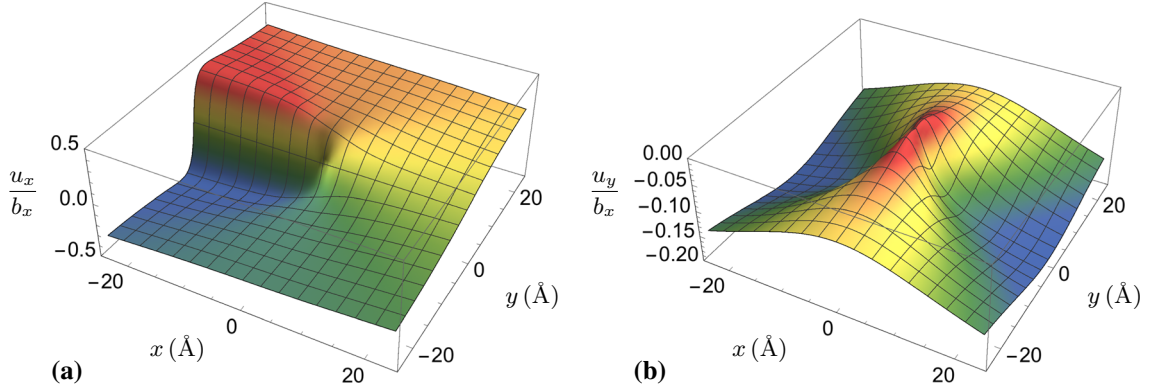


Fig. 9 Displacement fields of an edge dislocation near the dislocation line: **a** u_x and **b** u_y

gives

$$u_x = \frac{b_x}{2\pi} \left[\arctan \frac{y}{x} + \pi H(-x) \operatorname{sgn}(y) + \partial_y \int_x^\infty K_0(\sqrt{X^2 + y^2/\ell_2}) dX \right. \\ \left. + \frac{xy}{r^2} \left(1 - \frac{4\ell_2^2}{r^2} + 2K_2(r/\ell_2) \right) - \frac{1-2\nu}{2(1-\nu)} \frac{xy}{r^2} \left(1 - \frac{4\ell_1^2}{r^2} + 2K_2(r/\ell_1) \right) \right], \quad (94)$$

$$u_y = -\frac{b_x}{4\pi} \left[\frac{1-2\nu}{1-\nu} \left\{ \ln r + K_0(r/\ell_1) - \frac{x^2 - y^2}{r^2} \left(1 - \frac{4\ell_1^2}{r^2} + 2K_2(r/\ell_1) \right) \right\} \right. \\ \left. + \frac{x^2 - y^2}{r^2} \left(1 - \frac{4\ell_2^2}{r^2} + 2K_2(r/\ell_2) \right) \right], \quad (95)$$

where ν is the Poisson ratio. The displacement fields (94) and (95) are plotted in Fig. 9a, b, respectively. Note that the displacement fields (94) and (95) are non-singular and smooth functions. The displacement fields (94) and (95) obtained in reduced strain gradient elasticity are in agreement with the displacement fields obtained in Mindlin's strain gradient elasticity (see [5,30]).

If we substitute the displacement fields (92) and (93) and the plastic distortion (89) into Eq. (5), a straightforward calculation gives the four non-vanishing components of the incompatible elastic distortion tensor

$$\beta_{xx} = -\frac{b_x}{4\pi(1-\nu)} \frac{y}{r^2} \left[(1-2\nu) + \frac{2x^2}{r^2} - 2(1-\nu) \left\{ \frac{3x^2 - y^2}{r^2} \left(\frac{4\ell_2^2}{r^2} - 2K_2(r/\ell_2) \right) - \frac{x^2 - y^2}{\ell_2 r} K_1(r/\ell_2) \right\} \right. \\ \left. + (1-2\nu) \left\{ \frac{3x^2 - y^2}{r^2} \left(\frac{4\ell_1^2}{r^2} - 2K_2(r/\ell_1) \right) - \frac{2x^2}{\ell_1 r} K_1(r/\ell_1) \right\} \right], \quad (96)$$

$$\beta_{yy} = -\frac{b_x}{4\pi(1-\nu)} \frac{y}{r^2} \left[(1-2\nu) - \frac{2x^2}{r^2} + 2(1-\nu) \left\{ \frac{3x^2 - y^2}{r^2} \left(\frac{4\ell_2^2}{r^2} - 2K_2(r/\ell_2) \right) - \frac{x^2 - y^2}{\ell_2 r} K_1(r/\ell_2) \right\} \right. \\ \left. - (1-2\nu) \left\{ \frac{3x^2 - y^2}{r^2} \left(\frac{4\ell_1^2}{r^2} - 2K_2(r/\ell_1) \right) + \frac{2y^2}{\ell_1 r} K_1(r/\ell_1) \right\} \right], \quad (97)$$

$$\beta_{xy} = \frac{b_x}{4\pi(1-\nu)} \frac{x}{r^2} \left[(3-2\nu) - \frac{2y^2}{r^2} - 2(1-\nu) \left\{ \frac{x^2 - 3y^2}{r^2} \left(\frac{4\ell_2^2}{r^2} - 2K_2(r/\ell_2) \right) + \frac{x^2 + 3y^2}{\ell_2 r} K_1(r/\ell_2) \right\} \right. \\ \left. + (1-2\nu) \left\{ \frac{x^2 - 3y^2}{r^2} \left(\frac{4\ell_1^2}{r^2} - 2K_2(r/\ell_1) \right) + \frac{2y^2}{\ell_1 r} K_1(r/\ell_1) \right\} \right], \quad (98)$$

$$\beta_{yx} = -\frac{b_x}{4\pi(1-\nu)} \frac{x}{r^2} \left[(1-2\nu) + \frac{2y^2}{r^2} + 2(1-\nu) \left\{ \frac{x^2 - 3y^2}{r^2} \left(\frac{4\ell_2^2}{r^2} - 2K_2(r/\ell_2) \right) - \frac{x^2 - y^2}{\ell_2 r} K_1(r/\ell_2) \right\} \right. \\ \left. - (1-2\nu) \left\{ \frac{x^2 - 3y^2}{r^2} \left(\frac{4\ell_1^2}{r^2} - 2K_2(r/\ell_1) \right) + \frac{2y^2}{\ell_1 r} K_1(r/\ell_1) \right\} \right]. \quad (99)$$

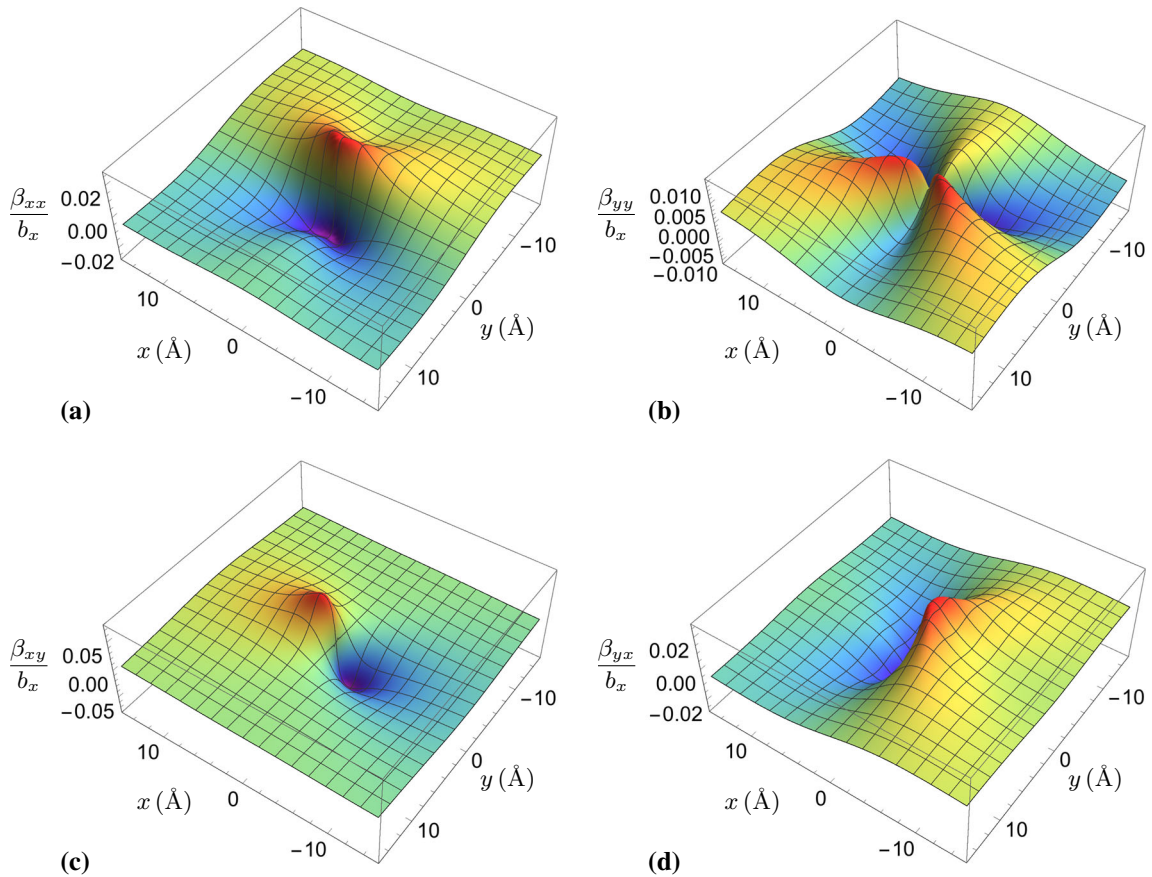


Fig. 10 Elastic distortion components of an edge dislocation near the dislocation line: **a** β_{xx} , **b** β_{yy} , **c** β_{xy} and **d** β_{yx}

The components of the elastic distortion tensor, Eqs. (96)–(99), are plotted in Figs. 10a–d and 11a–d. It can be seen that they are non-singular and zero at the dislocation line. The elastic distortion components (96), (97) and (99) obtained in reduced strain gradient elasticity are in full agreement with the corresponding ones obtained in Mindlin’s strain gradient elasticity (see [30]). Only the elastic distortion component (98) is slightly different because it depends only on 2 lengths scales (ℓ_1 , ℓ_2), whereas in Mindlin’s strain gradient elasticity the component β_{xy} depends on 3 lengths scales (ℓ_1 , ℓ_2 , ℓ_4) (see [30]). In the dislocation core region, the component β_{xy} obtained in the reduced strain gradient elasticity model is higher than the component β_{xy} in Mindlin’s strain gradient elasticity (see Fig. 11c). Using the values of the material parameters given in Table 1, the additional length in Mindlin’s first strain gradient elasticity is computed as $\ell_4 = 1.4405 \text{ \AA}$ (see also [30]).

The trace of the elastic distortion tensor gives the elastic dilatation which reads as

$$\beta_{ll} = -\frac{b_x(1-2\nu)}{2\pi(1-\nu)} \frac{y}{r^2} \left[1 - \frac{r}{\ell_1} K_1(r/\ell_1) \right], \quad (100)$$

depending on the longitudinal length ℓ_1 . The skew-symmetric part of the elastic distortion tensor gives the elastic rotation which reads as

$$\omega_{xy} = \frac{b_x}{2\pi} \frac{x}{r^2} \left[1 - \frac{r}{\ell_2} K_1(r/\ell_2) \right], \quad (101)$$

depending on the transverse length ℓ_2 .

Substituting the symmetric part of the elastic distortion tensor given in Eqs. (96)–(99) and the elastic dilatation (100) into the Hooke law (11), the non-vanishing components of the Cauchy stress tensor of an edge dislocation are calculated as

$$\sigma_{xx} = -\frac{\mu b_x}{2\pi(1-\nu)} \frac{y}{r^2} \left[\frac{3x^2 + y^2}{r^2} - \frac{2\nu r}{\ell_1} K_1(r/\ell_1) \right]$$

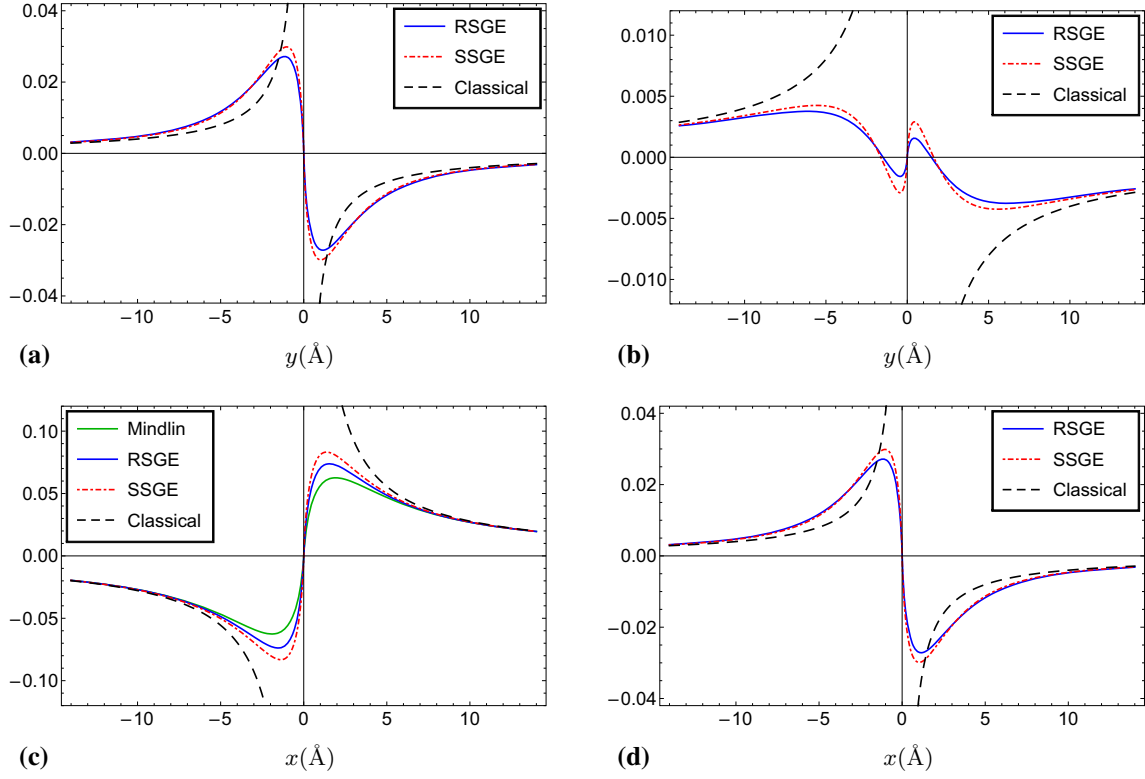


Fig. 11 Plots of the elastic distortion components of an edge dislocation in reduced strain gradient elasticity (RSGE), simplified strain gradient elasticity (SSGE), and classical elasticity (Classical): **a** β_{xx}/b_x , **b** β_{yy}/b_x , **c** β_{xy}/b_x , and **d** β_{yx}/b_x

$$\begin{aligned}
 & -2(1-\nu) \left\{ \frac{3x^2 - y^2}{r^2} \left(\frac{4\ell_2^2}{r^2} - 2K_2(r/\ell_2) \right) - \frac{x^2 - y^2}{\ell_2 r} K_1(r/\ell_2) \right\} \\
 & + (1-2\nu) \left\{ \frac{3x^2 - y^2}{r^2} \left(\frac{4\ell_1^2}{r^2} - 2K_2(r/\ell_1) \right) - \frac{2x^2}{\ell_1 r} K_1(r/\ell_1) \right\} \Bigg], \quad (102)
 \end{aligned}$$

$$\begin{aligned}
 \sigma_{yy} = & \frac{\mu b_x}{2\pi(1-\nu)} \frac{y}{r^2} \left[\frac{x^2 - y^2}{r^2} + \frac{2\nu r}{\ell_1} K_1(r/\ell_1) \right. \\
 & - 2(1-\nu) \left\{ \frac{3x^2 - y^2}{r^2} \left(\frac{4\ell_2^2}{r^2} - 2K_2(r/\ell_2) \right) - \frac{x^2 - y^2}{\ell_2 r} K_1(r/\ell_2) \right\} \\
 & \left. + (1-2\nu) \left\{ \frac{3x^2 - y^2}{r^2} \left(\frac{4\ell_1^2}{r^2} - 2K_2(r/\ell_1) \right) + \frac{2y^2}{\ell_1 r} K_1(r/\ell_1) \right\} \right], \quad (103)
 \end{aligned}$$

$$\begin{aligned}
 \sigma_{xy} = & \frac{\mu b_x}{2\pi(1-\nu)} \frac{x}{r^2} \left[\frac{x^2 - y^2}{r^2} \right. \\
 & - 2(1-\nu) \left\{ \frac{x^2 - 3y^2}{r^2} \left(\frac{4\ell_2^2}{r^2} - 2K_2(r/\ell_2) \right) + \frac{2y^2}{\ell_2 r} K_1(r/\ell_2) \right\} \\
 & \left. + (1-2\nu) \left\{ \frac{x^2 - 3y^2}{r^2} \left(\frac{4\ell_1^2}{r^2} - 2K_2(r/\ell_1) \right) + \frac{2y^2}{\ell_1 r} K_1(r/\ell_1) \right\} \right], \quad (104)
 \end{aligned}$$

$$\sigma_{zz} = -\frac{\mu\nu b_x}{\pi(1-\nu)} \frac{y}{r^2} \left[1 - \frac{r}{\ell_1} K_1(r/\ell_1) \right]. \quad (105)$$

The components of the Cauchy stress tensor, Eqs. (102)–(105), are plotted in Figs. 12a–d and 13a–d. It can be seen that they are non-singular. At the dislocation line, the stress is zero. The stress components (102), (103) and (105) obtained in reduced strain gradient elasticity are in full agreement with the corresponding

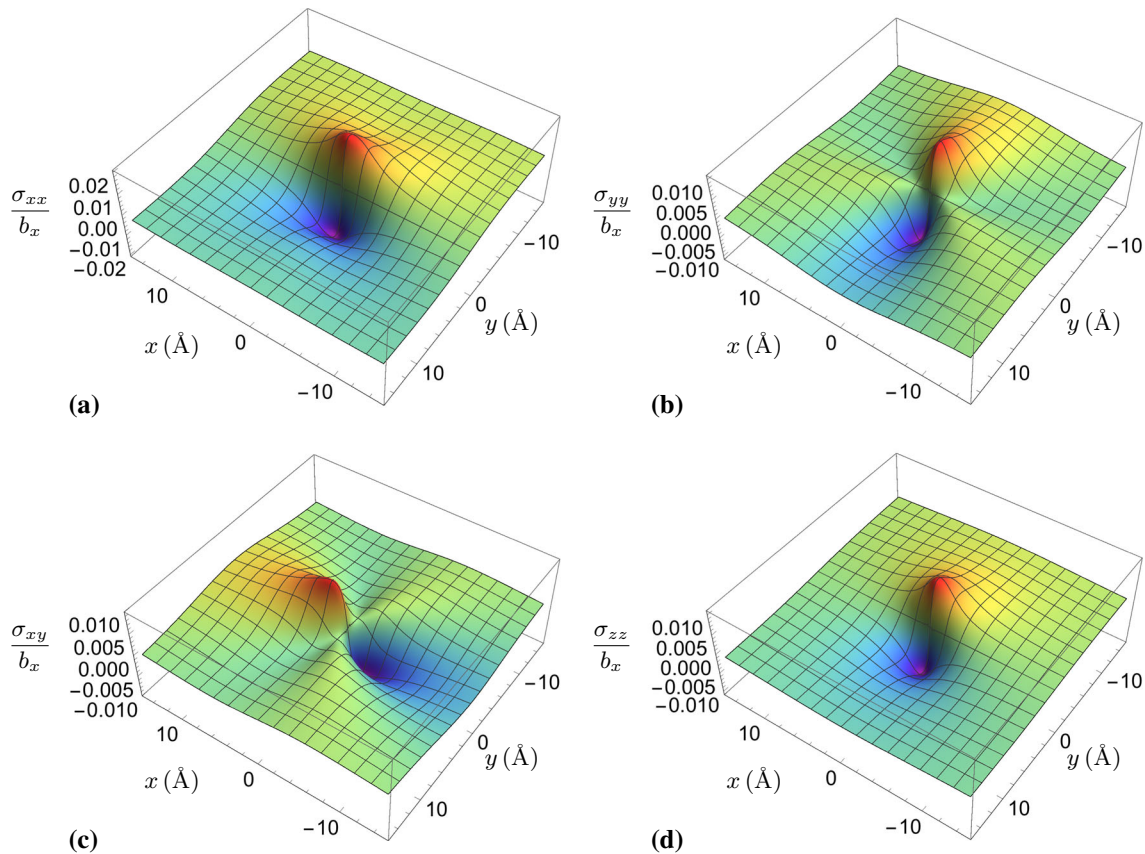


Fig. 12 Cauchy stress components of an edge dislocation near the dislocation line: **a** σ_{xx} , **b** σ_{yy} , **c** σ_{xy} and **d** σ_{zz}

stress components obtained in Mindlin's strain gradient elasticity (see [30]). Only the stress component (104) is slightly different because it depends only on 2 lengths scales, whereas in Mindlin's strain gradient elasticity the component σ_{xy} depends on 3 lengths scales (see [30]). In the dislocation core region, the component σ_{xy} obtained in the reduced strain gradient elasticity model is higher than the component σ_{xy} in Mindlin's strain gradient elasticity (see Fig. 13c).

3.3 Limit to simplified strain gradient elasticity

In this section, we carry out the limit from reduced strain gradient elasticity to simplified strain gradient elasticity for the fields of screw and edge dislocations. Since reduced strain gradient elasticity is a generalization of simplified strain gradient elasticity, the dislocation fields of the simplified strain gradient elasticity model must be recovered from the dislocation fields of the reduced strain gradient elasticity model. The limit towards simplified strain gradient elasticity reads [19,28]

$$a_1 = 0, \quad a_2 = \frac{\lambda \ell^2}{2}, \quad a_3 = 0, \quad a_4 = \mu \ell^2, \quad a_5 = 0 \quad (106)$$

and

$$\ell_1 = \ell_2 = \ell. \quad (107)$$

For a screw dislocation, the limit reads $\ell_2 = \ell$ in Eqs. (76), (77), (79), (81) and (82) which leads to known results in the literature (see, e.g., [9,11,19,24,30]). Therefore, the dislocation fields of a screw dislocation in reduced strain gradient elasticity are in agreement with the dislocation fields of a screw dislocation in simplified strain gradient elasticity.

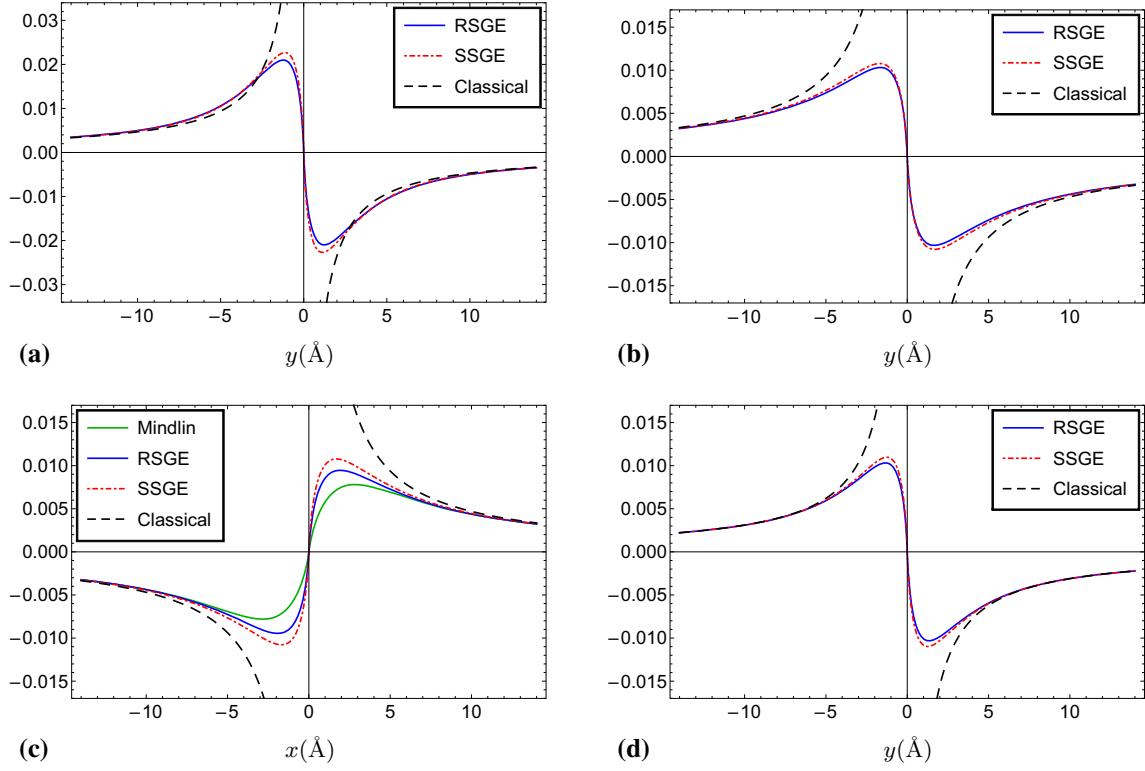


Fig. 13 Plots of the Cauchy stress components of an edge dislocation in reduced strain gradient elasticity (RSGE), simplified strain gradient elasticity (SSGE), and classical elasticity (Classical): **a** σ_{xx}/b_x , **b** σ_{yy}/b_x , **c** σ_{xy}/b_x , and **d** σ_{zz}/b_x

For an edge dislocation, the plastic distortion (89) and the dislocation density (90) reduce to formulas known in simplified strain gradient elasticity (see, e.g., [21,24,30]). The displacement fields (92) and (93) simplify to

$$u_x = \frac{b_x}{4\pi(1-\nu)} \left[2(1-\nu) \left(\arctan \frac{y}{x} + \pi H(-x) \operatorname{sgn}(y) + \partial_y \int_x^\infty K_0(\sqrt{X^2 + y^2}/\ell) dX \right) + \frac{xy}{r^2} \left(1 - \frac{4\ell^2}{r^2} + 2K_2(r/\ell) \right) \right], \quad (108)$$

$$u_y = -\frac{b_x}{4\pi(1-\nu)} \left[(1-2\nu) (\ln r + K_0(r/\ell)) + \frac{x^2 - y^2}{2r^2} \left(1 - \frac{4\ell^2}{r^2} + 2K_2(r/\ell) \right) \right]. \quad (109)$$

Equation (108) is in agreement with the displacement field given in [5,21,30]. Equation (109) agrees with the expression given in [5,10,21,30].

The incompatible elastic distortion fields (96)–(99) reduce to

$$\beta_{xx} = -\frac{b_x}{4\pi(1-\nu)} \frac{y}{r^2} \left[(1-2\nu) + \frac{2x^2}{r^2} - \frac{3x^2 - y^2}{r^2} \left(\frac{4\ell^2}{r^2} - 2K_2(r/\ell) \right) - \frac{2(y^2 - \nu r^2)}{\ell r} K_1(r/\ell) \right], \quad (110)$$

$$\beta_{yy} = -\frac{b_x}{4\pi(1-\nu)} \frac{y}{r^2} \left[(1-2\nu) - \frac{2x^2}{r^2} + \frac{3x^2 - y^2}{r^2} \left(\frac{4\ell^2}{r^2} - 2K_2(r/\ell) \right) - \frac{2(x^2 - \nu r^2)}{\ell r} K_1(r/\ell) \right], \quad (111)$$

$$\beta_{xy} = \frac{b_x}{4\pi(1-\nu)} \frac{x}{r^2} \left[(3-2\nu) - \frac{2y^2}{r^2} - \frac{x^2 - 3y^2}{r^2} \left(\frac{4\ell^2}{r^2} - 2K_2(r/\ell) \right) - \frac{2(y^2 + (1-\nu)r^2)}{\ell r} K_1(r/\ell) \right], \quad (112)$$

$$\beta_{yx} = -\frac{b_x}{4\pi(1-\nu)} \frac{x}{r^2} \left[(1-2\nu) + \frac{2y^2}{r^2} + \frac{x^2-3y^2}{r^2} \left(\frac{4\ell^2}{r^2} - 2K_2(r/\ell) \right) - \frac{2(x^2-\nu r^2)}{\ell r} K_1(r/\ell) \right], \quad (113)$$

which agree with the formulas given in [21,24,30]. The elastic distortion (96)–(99) obtained in reduced strain gradient elasticity, the elastic distortion (110)–(113) obtained in simplified strain gradient elasticity and the classical elastic distortion are plotted in Fig. 11 using the values of the length scales given in Table 1. It can be seen that for these values of the length scales, the elastic distortion in reduced strain gradient elasticity and the elastic distortion in simplified strain gradient elasticity are in good agreement even in the dislocation core region. Only the extremum values of the elastic distortion in the dislocation core region are slightly higher in simplified strain gradient elasticity than in reduced strain gradient elasticity for the used values of the length scales.

The stress fields (102)–(105) simplify to

$$\sigma_{xx} = -\frac{\mu b_x}{2\pi(1-\nu)} \frac{y}{r^4} \left[(3x^2 + y^2) - (3x^2 - y^2) \left(\frac{4\ell^2}{r^2} - 2K_2(r/\ell) \right) - \frac{2y^2 r}{\ell} K_1(r/\ell) \right], \quad (114)$$

$$\sigma_{yy} = \frac{\mu b_x}{2\pi(1-\nu)} \frac{y}{r^4} \left[(x^2 - y^2) - (3x^2 - y^2) \left(\frac{4\ell^2}{r^2} - 2K_2(r/\ell) \right) + \frac{2x^2 r}{\ell} K_1(r/\ell) \right], \quad (115)$$

$$\sigma_{xy} = \frac{\mu b_x}{2\pi(1-\nu)} \frac{x}{r^4} \left[(x^2 - y^2) - (x^2 - 3y^2) \left(\frac{4\ell^2}{r^2} - 2K_2(r/\ell) \right) - \frac{2y^2 r}{\ell} K_1(r/\ell) \right], \quad (116)$$

$$\sigma_{zz} = -\frac{\mu \nu b_x}{\pi(1-\nu)} \frac{y}{r^2} \left[1 - \frac{r}{\ell} K_1(r/\ell) \right], \quad (117)$$

which agree with the formulas given in [11,19,30]. The stress fields (102)–(105) obtained in reduced strain gradient elasticity, the stress fields (114)–(117) obtained in simplified strain gradient elasticity and the classical stress fields are plotted in Fig. 11 using the values of the length scales given in Table 1. It can be seen that for these values of the length scales, the stresses in reduced strain gradient elasticity and the stresses in simplified strain gradient elasticity are in good agreement even in the dislocation core region. The extremum values of the stress fields in the dislocation core region are slightly higher in simplified strain gradient elasticity than in reduced strain gradient elasticity for the used values of the length scales.

4 Conclusions

The reduced strain gradient elasticity model is developed in this paper. Reduced strain gradient elasticity is a strain gradient elasticity model involving two internal characteristic lengths in addition to the two Lamé parameters. It allows to eliminate elastic singularities and discontinuities and to interpret elastic size effects. Reduced strain gradient elasticity is a gradient model at a level of simplicity and complexity between simplified strain gradient elasticity and Mindlin's strain gradient elasticity. One advantage of reduced strain gradient elasticity is the fact that it possesses two internal characteristic lengths like Mindlin's strain gradient elasticity but less gradient-elastic constants than the five in Mindlin's gradient theory leading to simpler expressions for the total stress and double stress tensors. The reduced strain gradient elasticity model is the appropriate model if two length scales are needed but the full Mindlin strain gradient elasticity theory is too sophisticated for applications. Thus, reduced strain gradient elasticity theory contains most features of the full Mindlin strain gradient elasticity theory and can be used for many important applications at the Ångström-scale, but also as effective (gradient) theory with two independent length scales. Therefore, the reduced strain gradient elasticity model is a particular case of Mindlin's first strain gradient elasticity theory, and is a generalization of the simplified first strain gradient elasticity model to include two different characteristic length scale parameters.

In order to show the main advantages of the reduced strain gradient elasticity model, it has been employed to investigate straight dislocations. Exact analytical solutions for the displacement fields, elastic distortions, Cauchy stresses, plastic distortions and dislocation densities of screw and edge dislocations have been derived which demonstrate the elimination of any singularity from elastic and plastic fields at the dislocation line, except the dislocation density field possessing a logarithmic singularity at the dislocation line. The dislocation fields of a screw dislocation only depend on the characteristic transverse length ℓ_2 , whereas the dislocation fields of an edge dislocation depend on the characteristic longitudinal lengths ℓ_1 and the characteristic transverse length ℓ_2 . The most important length scale for the characteristic dislocation profiles of the displacement,

plastic distortion and dislocation density fields of screw and edge dislocations is the transverse length ℓ_2 . The dependence of the dislocation fields on the characteristic length scale parameters ℓ_1 and ℓ_2 is as follows. The fields of a screw dislocation only depend on the characteristic transverse length ℓ_2 in the following way:

- displacement field: $u_z = u_z(\mathbf{r}, \ell_2)$
- plastic distortion: $\beta_{zy}^P = \beta_{zy}^P(\mathbf{r}, \ell_2)$
- dislocation density: $\alpha_{zz} = \alpha_{zz}(\mathbf{r}, \ell_2)$
- incompatible elastic distortion: $\beta_{ij} = \beta_{ij}(\mathbf{r}, \ell_2)$
- Cauchy stress: $\sigma_{ij} = \sigma_{ij}(\mathbf{r}, \ell_2)$.

The fields of an edge dislocation depend on the characteristic longitudinal length ℓ_1 and the characteristic transverse length ℓ_2 in the following way:

- displacement field: $u_i = u_i(\mathbf{r}, \ell_1, \ell_2)$
- plastic distortion: $\beta_{xy}^P = \beta_{xy}^P(\mathbf{r}, \ell_2)$
- dislocation density: $\alpha_{xz} = \alpha_{xz}(\mathbf{r}, \ell_2)$
- incompatible elastic distortion: $\beta_{ij} = \beta_{ij}(\mathbf{r}, \ell_1, \ell_2)$
- Cauchy stress: $\sigma_{ij} = \sigma_{ij}(\mathbf{r}, \ell_1, \ell_2)$.

It is important to note that the main feature of the obtained solutions of screw and edge dislocations is the absence of any singularity in the displacement, elastic distortion, plastic distortion and stress fields due to the regularization in the framework of gradient elasticity.

Acknowledgements Markus Lazar gratefully acknowledges the grant obtained from the Deutsche Forschungsgemeinschaft (Grant No. LA1974/4-2).

Open Access This article is licensed under a Creative Commons Attribution 4.0 International License, which permits use, sharing, adaptation, distribution and reproduction in any medium or format, as long as you give appropriate credit to the original author(s) and the source, provide a link to the Creative Commons licence, and indicate if changes were made. The images or other third party material in this article are included in the article's Creative Commons licence, unless indicated otherwise in a credit line to the material. If material is not included in the article's Creative Commons licence and your intended use is not permitted by statutory regulation or exceeds the permitted use, you will need to obtain permission directly from the copyright holder. To view a copy of this licence, visit <http://creativecommons.org/licenses/by/4.0/>.

Funding Open Access funding enabled and organized by Projekt DEAL.

References

1. Admal, N.C., Marian, J., Po, G.: The atomistic representation of first strain-gradient elastic tensors. *J. Mech. Phys. Solids* **99**, 93–115 (2017)
2. Agiasofitou, E.K., Lazar, M.: Conservation and balance laws in linear elasticity of grade three. *J. Elast.* **94**, 69–85 (2009)
3. Altan, B.C., Aifantis, E.C.: On some aspects in the special theory of gradient elasticity. *J. Mech. Behav. Mater.* **8**, 231–282 (1997)
4. Delfani, M.R., Tavakol, E.: Uniformly moving screw dislocation in strain gradient elasticity. *Eur. J. Mech. A Solids* **73**, 349–355 (2019)
5. Delfani, M.R., Taaghi, S., Tavakol, E.: Uniform motion of an edge dislocation within Mindlin's first strain gradient elasticity. *Int. J. Mech. Sci.* **179**, 105701 (2020)
6. deWit, R.: Theory of disclinations IV. *J. Res. Natl. Bur. Stand.* **77A**, 607–658 (1973)
7. Edelen, D.G.B.: A correct, globally defined solution of the screw dislocation problem in the gauge theory of defects. *Int. J. Eng. Sci.* **34**, 81–86 (1996)
8. Eringen, A.C.: *Nonlocal Continuum Field Theories*. Springer, New York (2002)
9. Gutkin, MYu., Aifantis, E.C.: Screw dislocation in gradient elasticity. *Scr. Mater.* **35**, 1353–1358 (1996)
10. Gutkin, MYu., Aifantis, E.C.: Edge dislocation in gradient elasticity. *Scr. Mater.* **36**, 129–135 (1997)
11. Gutkin, MYu., Aifantis, E.C.: Dislocations in gradient elasticity. *Scr. Mater.* **40**, 559–566 (1999)
12. Hirth, J.P., Lothe, J.: *Theory of Dislocations*, 2nd edn. Wiley, New York (1982)
13. Jaunzemis, W.: *Continuum Mechanics*. The Macmillan Company, New York (1967)
14. Karlis, G.F., Charalambopoulos, A., Polyzos, D.: An advanced boundary element method for solving 2D and 3D static problems in Mindlin's strain-gradient theory of elasticity. *Int. J. Numer. Methods Eng.* **83**, 1407–1427 (2010)
15. Kröner, E.: *Kontinuumstheorie der Versetzungen und Eigenspannungen*. Springer, Berlin (1958)
16. Lardner, R.W.: Dislocations in materials with couple stress. *IMA J. Appl. Math.* **7**, 126–137 (1971)
17. Lazar, M.: An elastoplastic theory of dislocations as a physical field theory with torsion. *J. Phys. A Math. Gen.* **35**, 1983–2004 (2002)
18. Lazar, M.: Dislocations in the field theory of elastoplasticity. *Comput. Mater. Sci.* **28**, 419–428 (2003)
19. Lazar, M., Maugin, G.A.: Nonsingular stress and strain fields of dislocations and disclinations in first strain gradient elasticity. *Int. J. Eng. Sci.* **43**, 1157–1184 (2005)

20. Lazar, M., Maugin, G.A., Aifantis, E.C.: On dislocations in a special class of generalized elasticity. *Phys. Status Solidi B* **242**, 2365–2390 (2005)
21. Lazar, M., Maugin, G.A.: Dislocations in gradient elasticity revisited. *Proc. R. Soc. A* **462**, 3465–3480 (2006)
22. Lazar, M., Kirchner, H.O.K.: The Eshelby stress tensor, angular momentum tensor and dilatation flux in gradient elasticity. *Int. J. Solids Struct.* **44**, 2477–2486 (2007)
23. Lazar, M., Anastassiadis, C.: The gauge theory of dislocations: static solutions of screw and edge dislocations. *Philos. Mag.* **89**, 199–231 (2009)
24. Lazar, M.: The fundamentals of non-singular dislocations in the theory of gradient elasticity: dislocation loops and straight dislocations. *Int. J. Solids Struct.* **50**, 352–362 (2013)
25. Lazar, M.: On gradient field theories: gradient magnetostatics and gradient elasticity. *Philos. Mag.* **94**, 2840–2874 (2014)
26. Lazar, M.: Irreducible decomposition of strain gradient tensor in isotropic strain gradient elasticity. *Zeitschrift für angewandte Mathematik und Mechanik (ZAMM)* **96**, 1291–1305 (2016)
27. Lazar, M.: Non-singular dislocation continuum theories: Strain gradient elasticity versus Peierls–Nabarro model. *Philos. Mag.* **97**, 3246–3275 (2017)
28. Lazar, M., Po, G.: On Mindlin’s isotropic strain gradient elasticity: green tensors, regularization, and operator-split. *J. Micromech. Mol. Phys.* **3**(3 & 4), 1840008 (2018)
29. Lazar, M., Agiasofitou, E., Po, G.: Three-dimensional nonlocal anisotropic elasticity: a generalized continuum theory of Ångström-mechanics. *Acta Mech.* **231**, 743–781 (2020)
30. Lazar, M.: Incompatible strain gradient elasticity of Mindlin type: screw and edge dislocations. *Acta Mech.* **232**, 3471–3494 (2021)
31. Lazar, M., Agiasofitou, E., Böhlke, T.: Mathematical modeling of the elastic properties of cubic crystals at small scales based on the Toupin–Mindlin anisotropic first strain gradient elasticity. *Continuum Mech. Thermodyn.* **34**, 107–136 (2022)
32. Lee, B.-J., Baskes, M., Kim, H., Koo Cho, Y.: Second nearest-neighbor modified embedded atom method potentials for bcc transition metals. *Phys. Rev. B* **64**, 184102 (2001)
33. Lee, B.-J.: Second nearest-neighbor modified embedded-atom-method (2NN MEAM) (2014). https://openkim.org/cite/MD_111291751625_001
34. Li, S., Wang, G.: *Introduction to Micromechanics and Nanomechanics*. World Scientific, Singapore (2008)
35. Maugin, G.A.: *Material Inhomogeneities in Elasticity*. Chapman and Hall, London (1993)
36. Mindlin, R.D.: Micro-structure in linear elasticity. *Arch. Ration. Mech. Anal.* **16**, 51–78 (1964)
37. Mindlin, R.D., Eshel, N.N.: On first strain gradient theory in linear elasticity. *Int. J. Solids Struct.* **4**, 109–124 (1968)
38. Mindlin, R.D.: Elasticity, piezoelectricity and crystal lattice dynamics. *J. Elast.* **2**, 217–282 (1972)
39. Mura, T.: *Micromechanics of Defects in Solids*, 2nd edn. Martinus Nijhoff, Dordrecht (1987)
40. Ortner, N., Wagner, P.: *Fundamental Solutions of Linear Partial Differential Operators*. Springer, Cham (2015)
41. Pellegrini, Y.-P.: Dynamic Peierls–Nabarro equations for elastically isotropic crystals. *Phys. Rev. B* **81**, 024101 (2010)
42. Po, G., Lazar, M., Admal, N.C., Ghoniem, N.: A non-singular theory of dislocations in anisotropic crystals. *Int. J. Plast.* **103**, 1–22 (2018)
43. Po, G., Admal, N.C., Lazar, M.: The Green tensor of Mindlin’s anisotropic first strain gradient elasticity. *Mater. Theory* **3**, 3 (2019)
44. Rogula, D.: Some basic solutions in strain gradient elasticity theory of an arbitrary order. *Arch. Mech.* **25**, 43–68 (1973)
45. Shodja, H.M., Zaheri, A., Tehranchi, A.: Ab initio calculations of characteristic lengths of crystalline materials in first strain gradient elasticity. *Mech. Mater.* **61**, 73–78 (2013)
46. Shodja, H.M., Moosavian, H., Ojaghnezhad, F.: Toupin–Mindlin first strain gradient theory revisited for cubic crystals of hexoctahedral class: analytical expression of the material parameters in terms of the atomic force constants and evaluation via ab initio DFT. *Mech. Mater.* **123**, 19–29 (2018)
47. Toupin, R.A., Grazis, D.C.: Surface effects and initial stress in continuum and lattice models of elastic crystals. In: Wallis, R.F. (ed.) *Proceedings of the International Conference on Lattice Dynamics*, pp. 597–602. Pergamon Press, Copenhagen (1964)
48. Zauderer, E.: *Partial Differential Equations of Applied Mathematics*. Wiley, New York (1983)